Published in final edited form as:
Cancer Res. 2012 July 1; 72(13): 3187–3195. doi:10.1158/0008-5472.CAN-12-0534.

Loss of fibroblast HIF-1α accelerates tumorigenesis

Jung-whan Kim[1], **Colin Evans**[3], **Alexander Weidemann**[4], **Norihiko Takeda**[5], **Yun Sok Lee**[2], **Christian Stockmann**[6], **Cristina Branco-Price**[3], **Filip Brandberg**[1], **Gustavo Leone**[7], **Michael C. Ostrowski**[8], and **Randall S. Johnson**[3,*]

[1]Molecular Biology Section, Division of Biological Sciences, University of California, San Diego, La Jolla, California 92093, USA

[2]Department of Medicine, Division of Endocrinology and Metabolism, University of California, San Diego, La Jolla, California 92093, USA

[3]Department of Physiology, Development and Neuroscience, University of Cambridge, Cambridge, UK

[4]Friedrich-Alexander-Universitat Erlangen-Nuremberg, 91054 Erlangen, Germany

[5]Department of Cardiovascular Medicine, University of Tokyo, Graduate School of Medicine, Tokyo, Japan

[6]Institut fur Physiologie, Universitat Duisburg-Essen, D-45122 Essen, Germany

[7]Department of Molecular Genetics, College of Biological Sciences, Ohio State University, Columbus, OH 43210 USA

[8]Department of Molecular and Cellular Biochemistry, College of Medicine, Ohio State University, Columbus, OH 43210 USA

Abstract

Solid tumors consist of malignant cells and associated stromal components, including fibroblastic cells that contribute to tumor growth and progression. Although tumor fibrosis and aberrant vascularization contribute to the hypoxia often found in advanced tumors, the contribution of hypoxic signaling within tumor-associated fibroblasts to tumorigenesis remains unknown. In this study, we used a fibroblast-specific promoter to create mice in which key hypoxia regulatory genes, including *VHL*, *HIF-1*α, *HIF-2*α and *VEGF-A*, were knocked out specifically in tumor stromal fibroblasts. We found that loss of *HIF-1*α and its target gene *VEGF-A* accelerated tumor growth in murine model of mammary cancer. HIF-1α and VEGF-A loss also led to a reduction in vascular density and myeloid cell infiltration, which correlated with improved tumor perfusion. Together, our findings indicate that the fibroblast HIF-1α response is a critical component of tumor vascularization.

[*]**Correspondence: Randall S. Johnson**, Department of Physiology, Development & Neuroscience, University of Cambridge, Downing Street, Cambridge CB2 3EG, rsj33@cam.ac.uk.

The authors declare no conflict of interest

Keywords

fibroblast; hypoxia; hypoxia-inducible factor-1

INTRODUCTION

Tumor-associated stromal alterations influence the tumor microenvironment and significantly contribute to tumor growth and progression (1). Recently, it has also become clear that stroma co-evolves with tumor cells (2, 3), and that stromal fibroblasts are a prominent cell type in that process (4, 5). Unlike fibroblasts residing in normal tissues, tumor-associated fibroblasts exhibit distinctive tumor-promoting features: they release growth and angiogenic factors, recruit inflammatory cells, and remodel extracellular matrix (6–11).

Hypoxia, or low oxygen tension, is a significant characteristic of the tumor microenvironment. An inadequate blood supply to tumor tissue frequently results in the formation of hypoxic and necrotic regions. This in turn triggers the expression of hypoxia-inducible factors (HIFs)(12, 13). HIFs are heterodimeric helix-loop-helix transcription factors that are composed of two subunits: a constitutively expressed HIF-β subunit, and an oxygen dependent HIF-α subunit. The HIF-α proteins are post-translationally regulated by oxygenation (14–16), through a complex containing the pVHL tumor suppressor (17).

Virtually all rapidly growing solid tumors contain multiple transient or chronic areas of severe hypoxia (oxygen tensions of less than 1%), and HIF-α levels are highly correlated with other prognostic markers of cancer, mortality, and metastasis (18–20). To determine how hypoxic signaling in tumor-associated fibroblasts affects tumorigenesis, a series of fibroblast-specific conditional knockout mice was created utilizing an FSP-cre strain (6, 10, 21, 22). It was found that ablation of *Hif-1*α in stromal fibroblasts enhanced both tumor growth and perfusion while reducing vascular density. Fibroblast-specific deletion of *VEGF-A* had similar effects, indicating that hypoxic signaling and VEGF-A expression in stromal fibroblasts is an important aspect of solid tumor progression.

MATERIALS AND METHODS

Cell Culture

Mammary epithelial carcinoma cells from female, FVB strain mice carrying the MMTV-PyMT transgene (23, 24) were isolated by digestion of advanced mammary tumors with collagenase and hyaluronidase. Cells were cultured in DMEM with 10% fetal bovine serum and 1% penicillin-streptomycin in a humidified incubator with 5% carbon dioxide. To isolate tumor-associated fibroblasts, digested cell suspensions from late stage tumors were plated on a petri (bacterial culture) dish; cells adherent within an hour were harvested for genomic DNA analysis.

Transgenic Mice

Mice in FVB background harboring an oncogenic Polyoma virus middle T transgene under the control of the promoter of an murine Moloney virus (MMTV) long terminal repeat (23, 24) were bred to mice carrying loxP recombinase recognition sites in the *Hif-1*α, *HIF-2*α, *VHL* or *VEGF-A* genes (25–28). To induce fibroblast genetic ablation, mice with homozygous recombinase site-flanked alleles were bred to mice expressing Cre recombinase driven by the *fsp1* promoter(6, 10, 21, 22). MMTV-PyMT transgenic mice in these backgrounds were then generated by breeding. All mice were backcrossed to a more than tenth-generation congenic FVB background.

Tissue Processing, Histology, Immunohistochemistry, and Immunofluorescence

Tumor-bearing mice were asphyxiated with CO_2 and perfused with PBS plus 5mM EDTA followed by 4% paraformaldehyde (PFA). Tumors were removed and further fixed with 4% PFA for 24 hours followed by embedding in paraffin. Deparaffinized and rehydrated 5-μm sections were stained for hematoxylin and eosin (H&E) and Masson's trichrome, and immunostained with the following primary antibodies: monoclonal anti-HIF-1α (Cayman), biotinylated mouse anti-PCNA (BD Pharmingen), rat anti-CD34 (abcam), rat anti-F4/80 (Serotec), mouse anti-αSMA (Chemicon), and rabbit anti-FSP1 (Millipore). Vectastain ABC (Vector Lab), EnVision kit, or CSA Kit (Dako) with DAB substrate were used to visualize primary antibody binding according to manufacturer's instructions.

Quantitative Image Analysis

Immunostained images were captured by Leica DMR microscope and SPOT RT camera (Diagnostic Instruments Inc.) and positive staining was quantified as described previously (29, 30).

Detection of Hypoxia by Pimonidazole

Hypoxyprobe-1 kit (HPI, Inc.) was used to visualize regions of hypoxia according to manufacturer's instructions. Briefly, pimonidazole hydrochloride (60mg/kg body weight) was injected intraperitoneally 90 minutes prior to sacrifice. Pimonidazole adducts were detected by a 1MAb1 mouse monoclonal antibody.

Determination of Vascular Permeability by Evans Blue Dye

Evans blue dye (100 μL of 0.5%) was injected intravenously 30 minutes before sacrifice. Tumors (0.5g) were incubated in formamide for 24 hours at 37°C to quantify vascular permeability. Absorbance of extracted Evans blue dye was measured using a spectrophotometer at 620nm.

Immunoprecipitation and Immunoblotting

PyMT mammary tumors were lysed in T-PER tissue protein extraction reagent (Thermo Scientific) according to manufacturer's instructions. VEGFR2 was immunoprecipitated by incubating 1mg of total lysate with rabbit anti-VEGFR2 (55B11; Cell Signaling). Immunoprecipitated VEGFR2 was probed by immunoblotting for HRP-conjugated anti-phosphotyrosine (4G10; Millipore) to detect phosphorylated VEGFR2 or for anti-VEGFR2

(Santa Cruz Biotechnology) to detect total VEGFR2. To quantify phosphorylated to total VEGFR2 ratios, immunoblot PVDF membranes were scanned with a Typhoon fluorescence scanner and the signals determined using ImageQuant software.

RNA, Genomic DNA and qPCR

Total RNA was isolated from mammary tumors using TRIzol reagent (Invitrogen) and subjected to one-step quantitative RT-PCR (Applied Biosystems) to determine *VEGF-A* mRNA levels.

To determine the deletion efficiency of *HIF-1*α in stromal fibroblasts and gene expression in macrophages, genomic DNA and total RNA were extracted from thioglycollate-driven peritoneal macrophages and F4/80-positive tumor-associated macrophages isolated by magnetic beads (Stem Cell Technology). Quantitative PCR (Applied Biosystems) was performed using specific primers and probes (supplementary Table 1 for sequences).

Subcutaneous Tumor Growth

Mammary epithelial carcinoma cells (1×10^7 cells) were injected subcutaneously in accordance with institutional IACUC-approved protocols. Total tumor volume was calculated by the formula; volume = $(\text{width})^2 \times \text{length}/2$.

Statistical Analysis

Unpaired Student's *t*-tests were used for statistical analyses. Data is expressed as mean +/− SEM unless otherwise stated.

RESULTS

Specificity of Genetic Ablation in Fibroblasts

Deletion in fibroblasts employed mice with various conditional alleles and mice that express Cre recombinase under the control of the fsp1 promoter (*fsp1-cre*) (6, 10, 21, 22). These mice were bred into mice with the transgenic polyoma middle T gene (*PyMT*) under the control of the promoter of the mouse mammary tumor virus (MMTV) long terminal repeat: these develop advanced epithelial carcinomas in all mammary glands by the age of 15 weeks when on the FVB strain background (all mice in this study were maintained and evaluated in the FVB strain) (23, 24).

Pimonidazole staining demonstrated regions of hypoxia (oxygen tension of less than 10mmHg or ~2%) in stromal and malignant epithelial areas in this tumor type (Fig. 1A). To determine the efficacy of deletion in fibroblasts, tumors from WT mammary tumor-bearing mice were isolated and cell suspensions from were placed on a non-treated sterile polystyrene surface, followed by harvesting of adherent cells within an hour. This procedure enriches for fibroblasts, and quantitative PCR analysis of genomic DNA from this population showed an approximate rate of deletion of 50% (Fig. 1B). This was likely an underrepresentation of the total deletion efficiency, due to the relative impurity of this population of cells. As other transgenic alleles of *fsp-cre* have been reported to induce deletion in myeloid cells, an analysis of peritoneal macrophages from mutant mice was

carried out; this showed no evidence of deletion of conditional alleles (Supplementary Fig. 1A–C), indicating that this population of macrophages is not affected by the expression of this allele.

Deletion of HIF-1α alone in Fibroblasts Accelerates Mammary Tumor Growth and Progression

To determine how mammary tumor progression is influenced by fibroblast-specific deletion of HIF pathway factors, total mammary tumor mass was analyzed from mice bearing mutant alleles of *HIF-1*α, *HIF-2*α, and a negative regulator of *HIF-*α's, the *VHL* tumor suppressor gene (25–28). These analyses found no difference in rate of tumor progression in the *VHL* deletion and *HIF-2*α deletion animals; however, tumor mass was found to be significantly greater in *HIF-1*α mutant mice relative to control mice carrying the *MMTV-PyMT* transgene at 15 weeks of age (Fig. 2A, Supplementary Fig. 2A and Supplementary Fig. 3A–B).

To confirm these latter findings in a subcutaneous tumor model, syngeneic mammary epithelial tumor cells were injected into WT and fibroblast *Hif-1*α-null mice. Tumor growth was again significantly accelerated in fibroblast *Hif-1α*-null mice compared with WT controls (Fig. 2B and Supplementary Fig. 2B), suggesting that the pro-tumorigenic effect of *Hif-1*α deletion in fibroblasts is not restricted to the transgenic mammary tumor model.

Enhanced tumor growth in fibroblast *Hif-1*α-null mice was associated with greater tumor cell proliferation, as determined by proliferating cell nuclear antigen (PCNA) staining (Fig. 2C–D). Histological tumor stage analysis was performed as previously described (23), and revealed a greater level of advanced carcinoma in fibroblast *Hif-1*α-null tumors, and a greater level of pre-malignant hyperplasia and adenoma in WT tumors (Fig. 2E–F). These data suggest that deletion of *Hif-1*α in fibroblasts promotes tumorigenic progression.

Deletion of HIF-1α in Fibroblasts reduces tumor vascular density

As shown in many studies, e.g., (31), advanced malignancy is typically accompanied by high vessel density and a distinctive and generally abnormal vessel structure, characterized by spatially disorganized, highly dilated, and tortuous blood vessels (Fig 3A). In transgenic mammary tumors from animals lacking fibroblast *Hif-1*α, vascular structures have a reduced density (Fig. 3B–D). This relatively diminished microvasculature was also seen in subcutaneous tumors created via injection of mammary tumor cell lines into fibroblast *Hif-1*α-null mutants relative to wild type mice (Fig. 3E–F).

Although levels of *VEGF-A* mRNA, as determined by qPCR, were similar in WT and fibroblast *Hif-1*α-null mammary tumors (Fig. 3G), activation of the key VEGF receptor, VEGFR2, was decreased in fibroblast *Hif-1*α-null mammary tumors when compared with WT controls (Fig. 3H). Quantitative analysis showed a reduced ratio of phosphorylated VEGFR2 to total VEGFR2 in fibroblast *Hif-1*α-null mammary tumors versus tumor extract from WT control mice (Fig. 3I). These data suggest that deletion of fibroblast *Hif-1*α suppresses VEGFR2 signaling, without altering the total *VEGF-A* levels in mammary tumors, perhaps acting through localized alterations in VEGF-A signaling.

Tumor vasculature often has reduced levels of pericytes, which provide structural and functional support for vessel-lining endothelial cells. Representative double immunofluorescence staining for CD34 and the pericyte marker α-smooth muscle actin (αSMA) indicates that fibroblast *Hif-1*α-null tumors contain more αSMA-positive blood vessels than wild type control tumors (Supplementary Fig. 4A). Consistently, mRNA expression of the pericyte markers, PDGFR and αSMA, is elevated in total lysates of fibroblast *Hif-1*α-null tumors relative to levels seen in WT control tumors (Supplementary Fig. 4B).

Deletion of HIF-1α in Fibroblasts Improves Blood Perfusion

To determine whether the vasculature in fibroblast *Hif-1*α-null tumors was functionally altered, tumors in fibroblast *Hif-1*α-null tumors and those derived from WT controls were stained with the hypoxia marker pimonidazole: levels of this indicator were decreased in fibroblast *Hif-1*α-null tumors compared with WT controls (Fig. 4A and B), indicating improved perfusion and decreased tumor hypoxia.

Tumor blood vessel permeability was also reduced in fibroblast *Hif-1*α-null tumors; intravenous injection of Evans blue dye, which can be used to evaluate vascular permeability, showed significantly reduced levels of the dye had leaked from subcutaneous tumors in fibroblast *Hif-1*α-null mice, relative to the levels seen in tumor-bearing WT control mice (Fig. 4C).

Deletion of HIF-1α in Fibroblasts Attenuates Tumor-associated Macrophage Infiltration

Numerous studies have previously demonstrated that infiltration of macrophages is a characteristic of tumor progression in many cancers, especially during the malignant transition that accompanies the “angiogenic switch” (32, 33). To determine the effect of fibroblast-specific *Hif-1*α deletion on tumor-associated macrophage recruitment, immunostaining for the macrophage marker F4/80 was carried out (Fig. 5A–D) on transgenically-induced mammary tumors from fibroblast *Hif-1*α-null mice and those from WT controls. This assay showed a significant decrease in tumor associated macrophages in fibroblast *Hif-1*α-null mutant tumors, and suggests that loss of stromal fibroblast *Hif-1α* attenuates tumor-associated macrophage infiltration.

Deletion of VEGF-A in fibroblasts results in increased subcutaneous tumor growth

Given that VEGF-A is chemotactic for macrophages in mammary tumors, and that blocking VEGF-A activity normalizes tumor vasculature (29, 34–37), it was important to determine whether fibroblastic *VEGF-A* expression is also linked to acceleration of tumorigenesis. Following injection of mammary epithelial tumor cells, it was found that subcutaneous tumor masses were significantly greater in fibroblast *VEGF-A* null mice compared with WT controls (Fig. 6A–B). It was also found that when fibroblast *VEGF-A* null mice carried the transgenic MMTV-PyMT transgene mammary tumor blood vessels exhibited decreased microvessel density compared with WT controls. This was associated with reduced vessel diameters (Fig. 6C, upper panel and Fig. 6D).

Targeted loss of *VEGF-A* in fibroblasts also reduced tumor-associated macrophage recruitment into transgenically induced mammary tumors (Fig. 6C, bottom panel and Fig. 6D) but did not affect total tumor mass at 15 weeks of age (Supplementary Fig. 3C).

DISCUSSION

Tumor-stromal cell interactions have been intensively investigated in the past several years, but are complex and remain undefined to a significant degree (3). The data presented here identifies stromal fibroblast HIF-1α signaling as a significant negative regulator of tumor development.

HIF-1α is generally regarded as a tumor-promoting transcription factor and targeted deletion of *Hif-1α* in malignant epithelial cells, endothelial cells or myeloid cells accordingly has been shown to suppress tumor growth (38–40). We show here, however, that deletion of *Hif-1*α or *VEGF-A* in fibroblasts enhances tumor growth.

Over-expression of angiogenic factors can lead to a deterioration of tumor vessels and result in a hyper-permeable and non-functional state (31). Blood vessels in fibroblast-null *Hif-1*α- or *VEGF-A*-null tumors showed evidence of decreased permeability and density, and tumors had reduced hypoxia and an increased level of growth and progression.

Tumor-associated macrophage infiltration is attenuated in stromal fibroblast-specific *Hif-1*α and *VEGF-A* null mammary tumors in the current study, suggesting that stromal fibroblast-derived HIF-1α or VEGF-A mediates at least in part the pro-angiogenic macrophage infiltration of tumors. We have previously shown that myeloid cell-specific deletion of *VEGF-A* normalizes tumor vasculature and enhances tumor growth (29), and earlier studies have demonstrated that infiltration of tumor-associated macrophages is required for tumor angiogenesis and metastatic dissemination (33, 41). It will be important to determine how the process of HIF-1α response in the fibroblast lineages targeted here influences more advanced aspects of tumorigenic progression, including those of invasion and metastasis. Further analysis may still reveal important roles for the HIF-α factors expressed by fibroblasts in processes such as pre-metastatic bone marrow recruitment of inflammatory cells.

In summary, this study demonstrates the importance of the HIF-1 response in fibroblasts for both macrophage recruitment and infiltration, and for induction of alterations in tumor vasculature, with resulting effects on tumor perfusion and progression. There are key links between fibroblast function and inflammatory response that in turn affect tumor vascularization. Thus, fibroblast HIF-1α response is likely a critical factor in the link between malignancy inflammation, and tumor progression.

Supplementary Material

Refer to Web version on PubMed Central for supplementary material.

Acknowledgments

We would like to thank Shelly Choi, Logan Stark and the UCSD histology core laboratory for technical assistance. This work was supported by NIH F32 NRSA post-doctoral fellowship (1F32CA157088-01) to J. Kim; NIH grants CA082515, CA118165 and Susan G. Komen grant K081021, as well as a Wellcome Trust Principal Research Fellowship, to R.S. Johnson.

References

1. Egeblad M, Nakasone ES, Werb Z. Tumors as organs: complex tissues that interface with the entire organism. Developmental cell. 2010; 18:884–901. [PubMed: 20627072]
2. Bissell MJ, Radisky D. Putting tumours in context. Nature reviews Cancer. 2001; 1:46–54.
3. Polyak K, Haviv I, Campbell IG. Co-evolution of tumor cells and their microenvironment. Trends in genetics : TIG. 2009; 25:30–38. [PubMed: 19054589]
4. Kalluri R, Zeisberg M. Fibroblasts in cancer. Nature reviews Cancer. 2006; 6:392–401.
5. Bhowmick NA, Neilson EG, Moses HL. Stromal fibroblasts in cancer initiation and progression. Nature. 2004; 432:332–337. [PubMed: 15549095]
6. Bhowmick NA, Chytil A, Plieth D, Gorska AE, Dumont N, Shappell S, et al. TGF-beta signaling in fibroblasts modulates the oncogenic potential of adjacent epithelia. Science. 2004; 303:848–851. [PubMed: 14764882]
7. Coussens LM, Werb Z. Inflammation and cancer. Nature. 2002; 420:860–867. [PubMed: 12490959]
8. Kraman M, Bambrough PJ, Arnold JN, Roberts EW, Magiera L, Jones JO, et al. Suppression of antitumor immunity by stromal cells expressing fibroblast activation protein-alpha. Science. 2010; 330:827–830. [PubMed: 21051638]
9. Orimo A, Gupta PB, Sgroi DC, Arenzana-Seisdedos F, Delaunay T, Naeem R, et al. Stromal fibroblasts present in invasive human breast carcinomas promote tumor growth and angiogenesis through elevated SDF-1/CXCL12 secretion. Cell. 2005; 121:335–348. [PubMed: 15882617]
10. Trimboli AJ, Cantemir-Stone CZ, Li F, Wallace JA, Merchant A, Creasap N, et al. Pten in stromal fibroblasts suppresses mammary epithelial tumours. Nature. 2009; 461:1084–1091. [PubMed: 19847259]
11. Erez N, Truitt M, Olson P, Arron ST, Hanahan D. Cancer-Associated Fibroblasts Are Activated in Incipient Neoplasia to Orchestrate Tumor-Promoting Inflammation in an NF-kappaB-Dependent Manner. Cancer cell. 2010; 17:135–147. [PubMed: 20138012]
12. Semenza GL, Roth PH, Fang HM, Wang GL. Transcriptional regulation of genes encoding glycolytic enzymes by hypoxia-inducible factor 1. J Biol Chem. 1994; 269:23757–23763. [PubMed: 8089148]
13. Semenza GL, Wang GL. A nuclear factor induced by hypoxia via de novo protein synthesis binds to the human erythropoietin gene enhancer at a site required for transcriptional activation. Mol Cell Biol. 1992; 12:5447–5454. [PubMed: 1448077]
14. Ivan M, Kondo K, Yang H, Kim W, Valiando J, Ohh M, et al. HIFalpha targeted for VHL-mediated destruction by proline hydroxylation: implications for O2 sensing. Science. 2001; 292:464–468. [PubMed: 11292862]
15. Jaakkola P, Mole DR, Tian YM, Wilson MI, Gielbert J, Gaskell SJ, et al. Targeting of HIF-alpha to the von Hippel-Lindau ubiquitylation complex by O2-regulated prolyl hydroxylation. Science. 2001; 292:468–472. [PubMed: 11292861]
16. Maxwell PH, Wiesener MS, Chang GW, Clifford SC, Vaux EC, Cockman ME, et al. The tumour suppressor protein VHL targets hypoxia-inducible factors for oxygen-dependent proteolysis. Nature. 1999; 399:271–275. [PubMed: 10353251]
17. Ohh M, Park CW, Ivan M, Hoffman MA, Kim TY, Huang LE, et al. Ubiquitination of hypoxia-inducible factor requires direct binding to the beta-domain of the von Hippel-Lindau protein. Nat Cell Biol. 2000; 2:423–427. [PubMed: 10878807]
18. Bos R, Zhong H, Hanrahan CF, Mommers EC, Semenza GL, Pinedo HM, et al. Levels of hypoxia-inducible factor-1 alpha during breast carcinogenesis. J Natl Cancer Inst. 2001; 93:309–314. [PubMed: 11181778]

19. Zhong H, De Marzo AM, Laughner E, Lim M, Hilton DA, Zagzag D, et al. Overexpression of hypoxia-inducible factor 1alpha in common human cancers and their metastases. Cancer research. 1999; 59:5830–5835. [PubMed: 10582706]
20. Semenza GL. Targeting HIF-1 for cancer therapy. Nat Rev Cancer. 2003; 3:721–732. [PubMed: 13130303]
21. Trimboli AJ, Fukino K, de Bruin A, Wei G, Shen L, Tanner SM, et al. Direct evidence for epithelial-mesenchymal transitions in breast cancer. Cancer research. 2008; 68:937–945. [PubMed: 18245497]
22. Strutz F, Okada H, Lo CW, Danoff T, Carone RL, Tomaszewski JE, et al. Identification and characterization of a fibroblast marker: FSP1. The Journal of cell biology. 1995; 130:393–405. [PubMed: 7615639]
23. Lin EY, Jones JG, Li P, Zhu L, Whitney KD, Muller WJ, et al. Progression to malignancy in the polyoma middle T oncoprotein mouse breast cancer model provides a reliable model for human diseases. Am J Pathol. 2003; 163:2113–2126. [PubMed: 14578209]
24. Guy CT, Cardiff RD, Muller WJ. Induction of mammary tumors by expression of polyomavirus middle T oncogene: a transgenic mouse model for metastatic disease. Mol Cell Biol. 1992; 12:954–961. [PubMed: 1312220]
25. Ryan HE, Poloni M, McNulty W, Elson D, Gassmann M, Arbeit JM, et al. Hypoxia-inducible factor-1 alpha is a positive factor in solid tumor growth. Cancer Res. 2000; 60:4010–4015. [PubMed: 10945599]
26. Gruber M, Hu CJ, Johnson RS, Brown EJ, Keith B, Simon MC. Acute postnatal ablation of Hif-2{alpha} results in anemia. Proc Natl Acad Sci U S A. 2007; 104:2301–2306. [PubMed: 17284606]
27. Haase VH, Glickman JN, Socolovsky M, Jaenisch R. Vascular tumors in livers with targeted inactivation of the von Hippel-Lindau tumor suppressor. Proc Natl Acad Sci U S A. 2001; 98:1583–1588. [PubMed: 11171994]
28. Gerber HP, Hillan KJ, Ryan AM, Kowalski J, Keller GA, Rangell L, et al. VEGF is required for growth and survival in neonatal mice. Development. 1999; 126:1149–1159. [PubMed: 10021335]
29. Stockmann C, Doedens A, Weidemann A, Zhang N, Takeda N, Greenberg JI, et al. Deletion of vascular endothelial growth factor in myeloid cells accelerates tumorigenesis. Nature. 2008; 456:814–818. [PubMed: 18997773]
30. Stockmann C, Kerdiles Y, Nomaksteinsky M, Weidemann A, Takeda N, Doedens A, et al. Loss of myeloid cell-derived vascular endothelial growth factor accelerates fibrosis. Proceedings of the National Academy of Sciences of the United States of America. 2010; 107:4329–4334. [PubMed: 20142499]
31. De Bock K, Cauwenberghs S, Carmeliet P. Vessel abnormalization: another hallmark of cancer? Molecular mechanisms and therapeutic implications. Current opinion in genetics & development. 2011; 21:73–79. [PubMed: 21106363]
32. Lin EY, Pollard JW. Tumor-associated macrophages press the angiogenic switch in breast cancer. Cancer research. 2007; 67:5064–5066. [PubMed: 17545580]
33. Lin EY, Li JF, Gnatovskiy L, Deng Y, Zhu L, Grzesik DA, et al. Macrophages regulate the angiogenic switch in a mouse model of breast cancer. Cancer Res. 2006; 66:11238–11246. [PubMed: 17114237]
34. Sawano A, Iwai S, Sakurai Y, Ito M, Shitara K, Nakahata T, et al. Flt-1, vascular endothelial growth factor receptor 1, is a novel cell surface marker for the lineage of monocyte-macrophages in humans. Blood. 2001; 97:785–791. [PubMed: 11157498]
35. Kerber M, Reiss Y, Wickersheim A, Jugold M, Kiessling F, Heil M, et al. Flt-1 signaling in macrophages promotes glioma growth in vivo. Cancer research. 2008; 68:7342–7351. [PubMed: 18794121]
36. Tong RT, Boucher Y, Kozin SV, Winkler F, Hicklin DJ, Jain RK. Vascular normalization by vascular endothelial growth factor receptor 2 blockade induces a pressure gradient across the vasculature and improves drug penetration in tumors. Cancer research. 2004; 64:3731–3736. [PubMed: 15172975]

37. Winkler F, Kozin SV, Tong RT, Chae SS, Booth MF, Garkavtsev I, et al. Kinetics of vascular normalization by VEGFR2 blockade governs brain tumor response to radiation: role of oxygenation, angiopoietin-1, and matrix metalloproteinases. Cancer cell. 2004; 6:553–563. [PubMed: 15607960]

38. Doedens AL, Stockmann C, Rubinstein MP, Liao D, Zhang N, DeNardo DG, et al. Macrophage expression of hypoxia-inducible factor-1 alpha suppresses T-cell function and promotes tumor progression. Cancer research. 2010; 70:7465–7475. [PubMed: 20841473]

39. Liao D, Corle C, Seagroves TN, Johnson RS. Hypoxia-inducible factor-1alpha is a key regulator of metastasis in a transgenic model of cancer initiation and progression. Cancer Res. 2007; 67:563–572. [PubMed: 17234764]

40. Tang N, Wang L, Esko J, Giordano FJ, Huang Y, Gerber HP, et al. Loss of HIF-1alpha in endothelial cells disrupts a hypoxia-driven VEGF autocrine loop necessary for tumorigenesis. Cancer cell. 2004; 6:485–495. [PubMed: 15542432]

41. Lin EY, Nguyen AV, Russell RG, Pollard JW. Colony-stimulating factor 1 promotes progression of mammary tumors to malignancy. The Journal of experimental medicine. 2001; 193:727–740. [PubMed: 11257139]

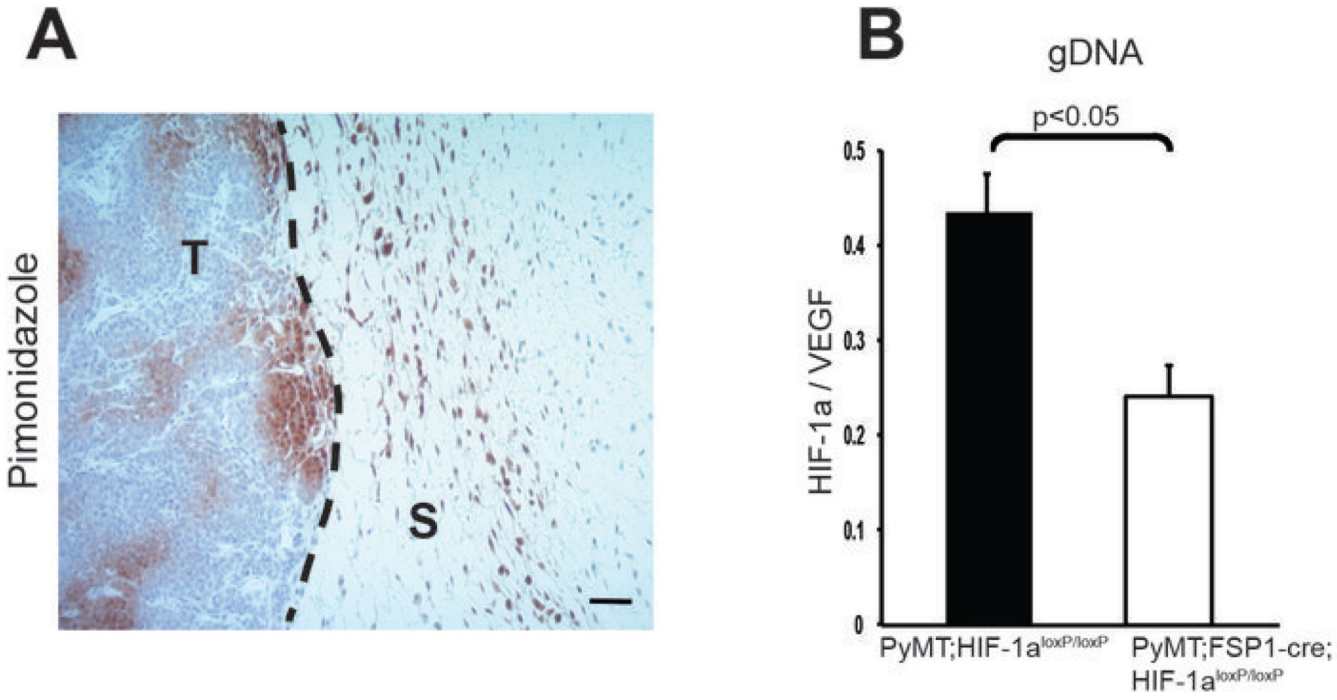

Figure 1. Targeted Deletion of *HIF-1α* in stromal fibroblasts

(A) Hypoxic areas (brown) in transgenically induced mammary tumors were detected by immunostaining for the hypoxia marker of bioreductivity, pimonidazole; scale bar, 100 μm. T, tumor; S, stroma. **(B)** Genomic DNA extracted from stromal fibroblasts isolated from WT and fibroblast *HIF-1α* null mammary tumors by culturing on petri dish were analyzed for the expression of *HIF-1α*. Genomic DNA level was normalized to *VEGF-A* genomic sequence as a non-deleted control for gene dosage.

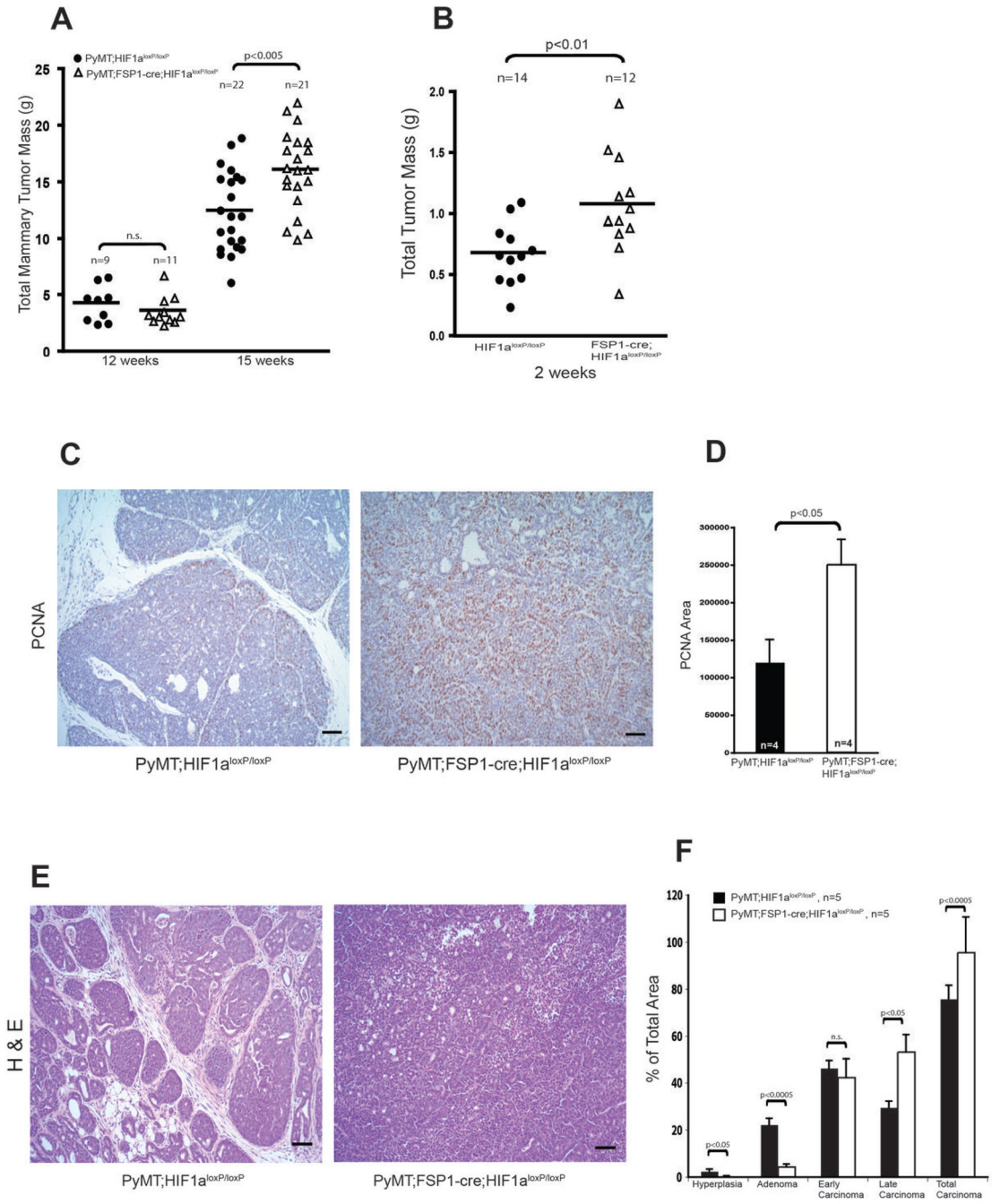

Figure 2. Deletion of Stromal Fibroblast *HIF-1α* Promotes Mammary Tumor Growth and Progression

(A) Total mammary tumor mass of WT (*PyMT;Hif-1α$^{loxp/loxp}$*) and fibroblast *HIF-1α* null (*PyMT;Fsp-cre;Hif-1α$^{loxp/loxp}$*) mice measured at the indicated age. **(B)** Total isograft tumor burden at 2 weeks post-subcutaneous injection of tumor cells into WT (*Hif-1α$^{loxp/loxp}$*) and fibroblast *HIF-1α* null (*Fsp-cre;Hif-1α$^{loxp/loxp}$*) mice. **(C)** Immunostaining for PCNA in tumor sections from 15-week-old WT (*PyMT;Hif-1α$^{loxp/loxp}$*) and fibroblast *HIF-1α* null (*PyMT;Fsp-cre;Hif-1α$^{loxp/loxp}$*) mice; scale bars: 100μm. **(D)** Quantification of PCNA-

positive areas in sections represented in Fig. 2C. **(E)** Representative images of H&E stained mammary tumors collected from 15-week-old WT (*PyMT;Hif-1α*$^{loxp/loxp}$) and fibroblast *HIF-1α* null (*PyMT;Fsp-cre;Hif-1α*$^{loxp/loxp}$) mice; scale bars: 100μm. **(F)** Histological stage distribution of mammary tumors from 15-week-old WT (*PyMT;Hif-1α*$^{loxp/loxp}$) and fibroblast *HIF-1α* null (*PyMT;Fsp-cre; Hif-1α*$^{loxp/loxp}$) mice.

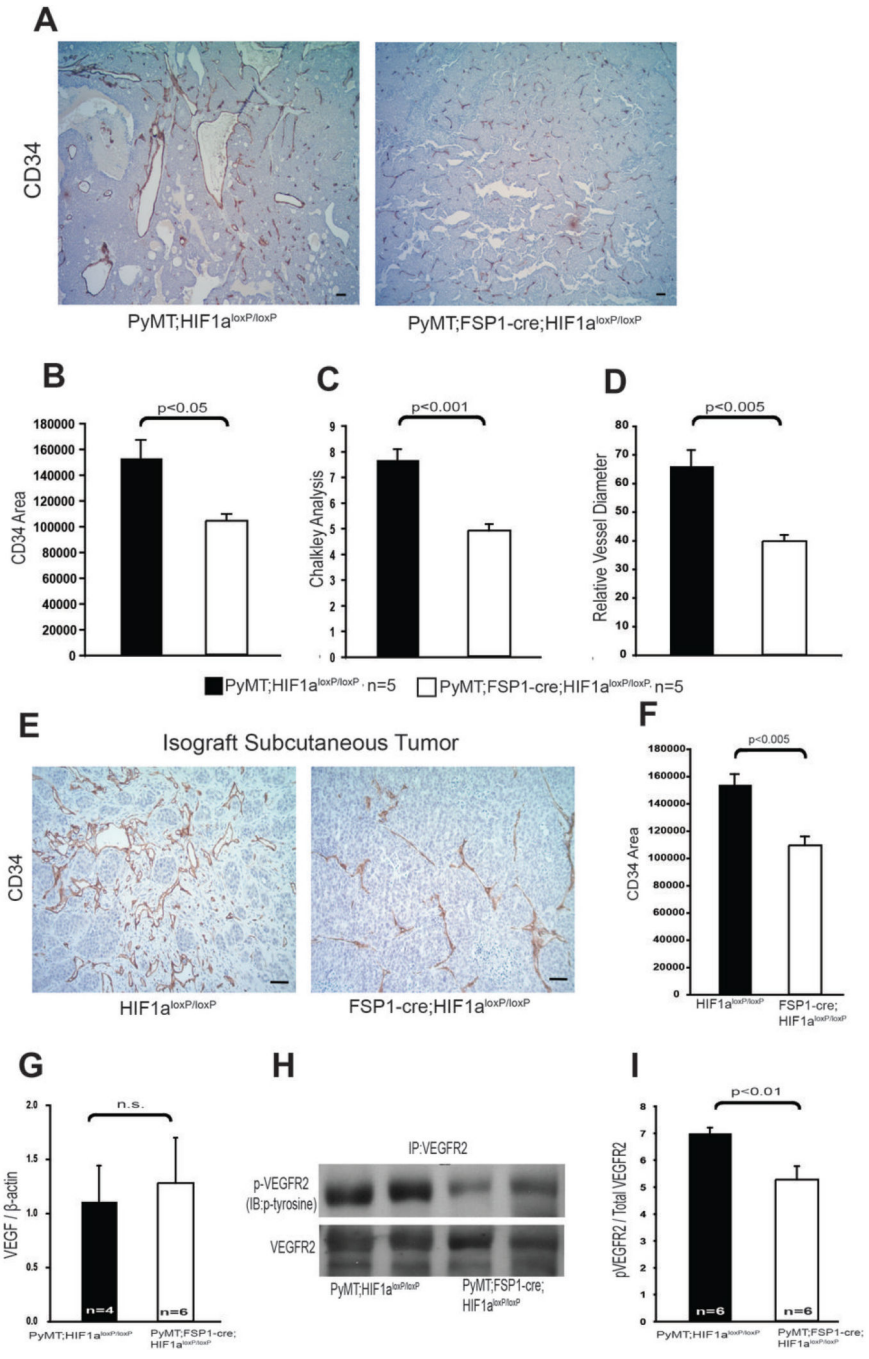

Figure 3. Ablation of *HIF-1α* in fibroblasts reduces tumor vascularization

(A) Tumor vasculature was visualized by CD34 immunostaining of tumor sections collected from 15-week-old WT (*PyMT;Hif-1α$^{loxp/loxp}$*) and fibroblast *HIF-1α* null (*PyMT;Fsp-cre;Hif-1α$^{loxp/loxp}$*) mice; scale bars: 100μm. **(B)** Quantification of CD34-positive stained areas from the tumors in Fig 3A. **(C)** Quantification of blood vessel density determined by Chalkley analysis of the tumors described for Fig. 3A. **(D)** Quantification of blood vessel diameter in the tumors described for Fig. 3A. **(E)** Representative sections of CD34-stained isograft subcutaneous tumors collected 2 weeks post-injection of syngeneic mammary tumor

cells in WT (*PyMT;Hif-1*$\alpha^{loxp/loxp}$) and fibroblast *HIF-1*α null (*PyMT;Fsp-cre;Hif-1*$\alpha^{loxp/loxp}$) mice; scale bars: 100μm. **(F)** Quantification of CD34-positive stained area in tumors described in Fig. 3E. **(G)** Quantification of *VEGF-A* mRNA expression in mammary tumors. Values represent mean ratio of *VEGF-A* mRNA to β-*actin* mRNA ± SEM. **(H)** Representative immunoblot analysis of phosphotyrosine presence in immunoprecipitated VEGFR2, and total VEGFR2 in mammary tumor lysates. **(I)** Quantification of phosphotyrosine and VEGFR2 by measuring photon emission in the blots described in Fig. 3H. Values represent the mean ratio of phosphotyrosine to total VEGFR2 photon emission intensities ± SEM.

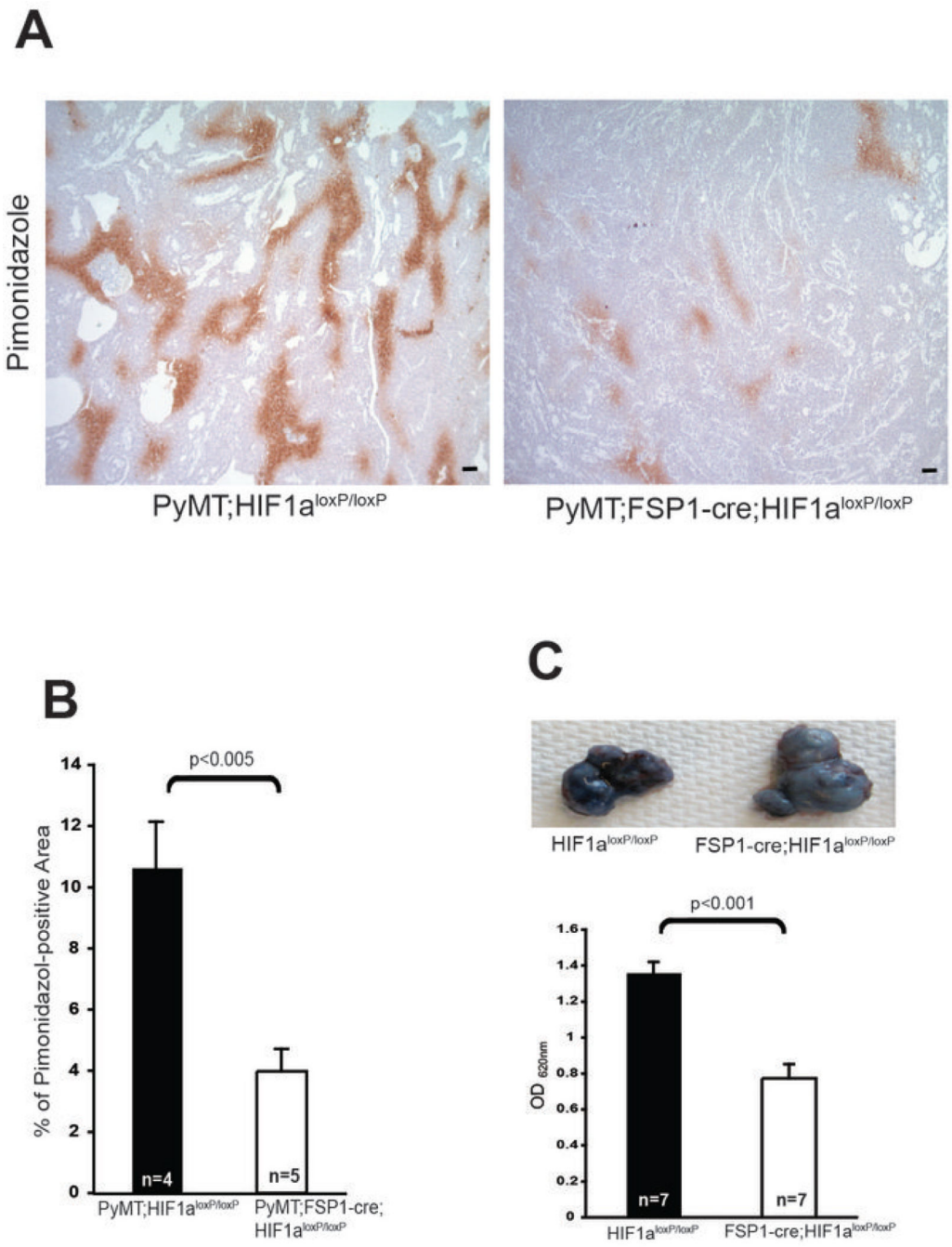

Figure 4. Targeted Deletion of *HIF-1α* in Fibroblasts reduces hypoxia

(A) Hypoxic areas in mammary tumor sections from 15-week-old WT (*PyMT;Hif-1α*$^{loxp/loxp}$) and fibroblast *HIF-1α* null (*PyMT;Fsp-cre;Hif-1α*$^{loxp/loxp}$) mice were visualized by immunostaining for the hypoxia marker pimonidazole; scale bar, 100 μm. **(B)** Quantification of pimonidazole staining in mammary tumors referred to in Fig. 4A. **(C)** Upper: Evans blue dye extravasation in subcutaneous tumors collected from WT (*PyMT;Hif-1α*$^{loxp/loxp}$) and fibroblast *HIF-1α* null (*PyMT;Fsp-cre; Hif-1α*$^{loxp/loxp}$) mice at 2 weeks post-injection of tumor cells. Lower: Quantification of extravasated Evans blue dye.

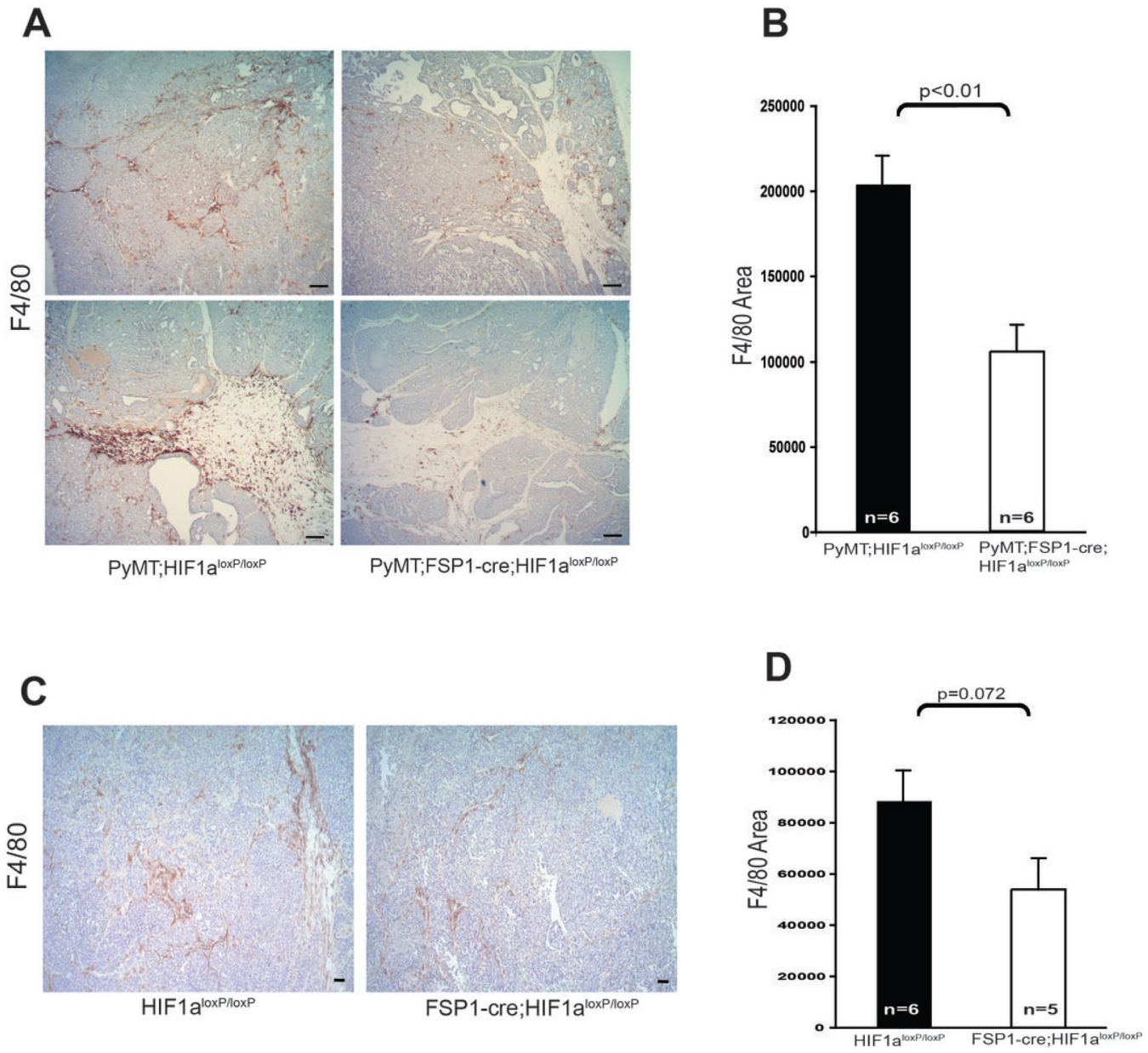

Figure 5. Fibroblast *Hif-1α* Deletion Attenuates Macrophage Infiltration in Mammary Tumors

(A) Representative mammary tumor sections from 15-week-old WT (*PyMT;Hif-1α$^{loxp/loxp}$*) and fibroblast *HIF-1α* null (*PyMT;Fsp-cre;Hif-1α$^{loxp/loxp}$*) mice, stained for the macrophage marker F4/80; scale bars: 100μm. **(B)** Quantification of F4/80-stained area in mammary tumors as in Fig. 5A. **(C)** Representative sections from subcutaneous tumors at 2 weeks post-injection of tumor cells in WT (*PyMT;Hif-1α$^{loxp/loxp}$*) and fibroblast *HIF-1α* null (*PyMT;Fsp-cre; Hif-1α$^{loxp/loxp}$*) mice stained for F4/80; scale bars: 100μm. **(D)** Quantification of F4/80 stained area in tumors described in Fig. 5C.

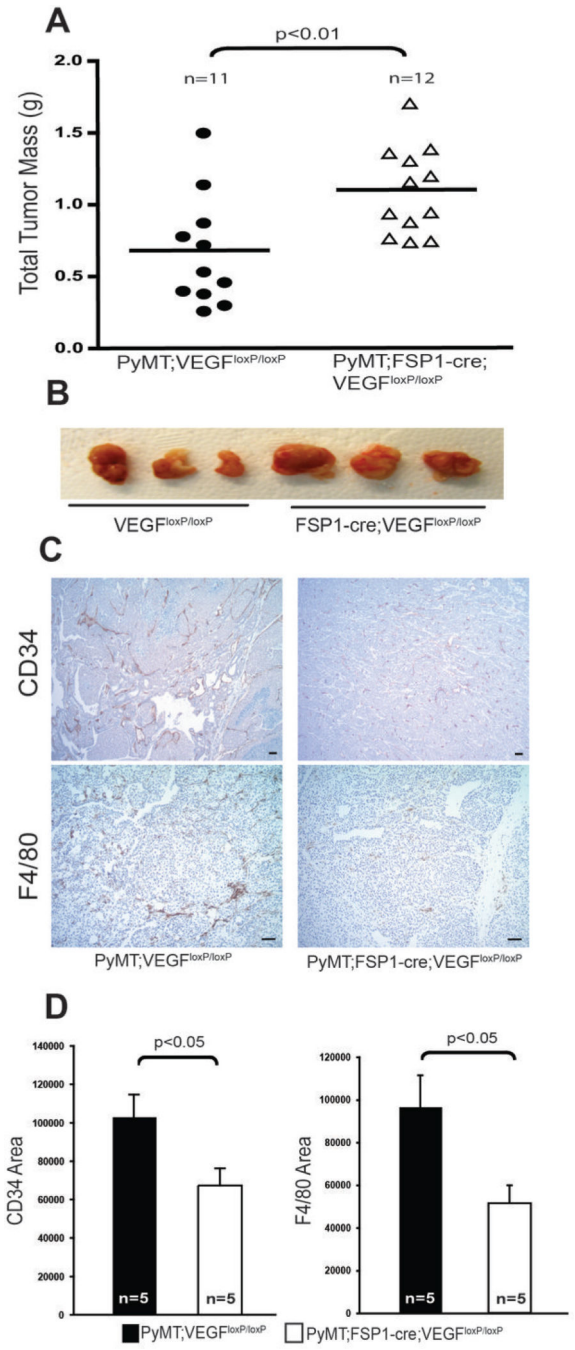

Figure 6. Deletion of *VEGF-A* in Fibroblasts Promotes Tumor Growth in syngeneic isografts

(A) Total isograft tumor mass at 2 weeks post-subcutaneous injection of tumor cells into WT (*Vegfa*$^{loxp/loxp}$) and fibroblast VEGF-Fibroblast A null (*Fsp-cre;Vegfa*$^{loxp/loxp}$) mice. **(B)** Representative image of isograft subcutaneous tumors harvested from WT (*Vegfa*$^{loxp/loxp}$) and fibroblast VEGF-A null (*Fsp-cre;Vegfa*$^{loxp/loxp}$) mice at 2 weeks post-injection of tumor cells. **(C)** Representative tumor sections from 15-week-old WT (*Vegfa*$^{loxp/loxp}$) and fibroblast VEGF-A null (*Fsp-cre;Vegfa*$^{loxp/loxp}$) mice stained for CD34

(upper panels) and F4/80 (bottom panels); scale bars: 100μm. **(D)** Quantification of CD34- (left) and F4/80- (right) stained area in tumors described in Fig. 6C.